Heliyon 10 (2024) e36321

Contents lists available at ScienceDirect

Heliyon

journal homepage: www.cell.com/heliyon

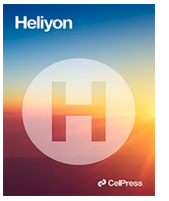

Research article

LncRNA PKD1P6 modulates ovarian granulosa cell survival of hyperandrogenic polycystic ovary syndrome by targeting miR-135b-5p and inhibiting ERK1/2 signaling

Weidong Zhou [a,*], Yikai Lian [a], Jiahao Chen [b], Teng Zhang [a], Wenjing Zhang [a], Ruofan Huang [b], Mengjie Yang [b], Xiaohong Yan [a], Qionghua Chen [b,**]

[a] *Reproductive Medicine Center, the First Affiliated Hospital of Xiamen University, School of Medicine, Xiamen University, Xiamen, Fujian, China*
[b] *Department of Obstetrics and Gynecology, the First Affiliated Hospital of Xiamen University, School of Medicine, Xiamen University, Xiamen, Fujian, China*

ARTICLE INFO

Keywords:
LncRNA PKD1P6
miR-135b-5p
Ovarian granulosa cell
MAPK pathway
Polycystic ovary syndrome

ABSTRACT

Polycystic ovary syndrome (PCOS) is the most common and multifactorial endocrine disease among women of reproductive age. Aberrant folliculogenesis is a common pathological characteristic of PCOS, but the underlying molecular mechanism remains unclear. Emerging evidence indicated that aberrant expression of long noncoding RNAs (lncRNAs) may contribute to the pathogenesis of PCOS. In this study, we found that lncRNA PKD1P6 expression was remarkably down-regulated in ovarian granulosa cells (GCs) of hyperandrogenic PCOS (HA-PCOS) patients and negatively correlated with serum testosterone (T) levels. We further showed that overexpression of PKD1P6 markedly reduced cell viability, attenuated DNA synthesis capacity, arrested the cell cycle at G0/G1 phase and promoted apoptosis of KGN cells. Exosomes derived from PKD1P6 overexpression cells exerted similar effects to PKD1P6 overexpression on the function of KGN cells. Mechanistically, PKD1P6 could act as a competing endogenous RNA (ceRNA) by directly binding with miR-135b-5p. Overexpression of PKD1P6 significantly suppressed ERK1/2 activation, whereas up-regulation of miR-135b-5p exerted an opposing effect. Additionally, excessive androgen was showed to diminish PKD1P6 expression while promote miR-135b-5p expression of PCOS models in vitro and vivo. Collectively, our findings delineate the clinical significance of PKD1P6 in HA-PCOS and the new regulatory mechanisms involved in abnormal folliculogenesis, providing a promising therapeutic target for HA-PCOS.

1. Introduction

Polycystic ovary syndrome (PCOS) is one of the most common endocrine disorders, affecting 10–15 % of women worldwide [1]. Based on the international evidence-based guidelines, PCOS is diagnosed by the Rotterdam criteria, which requires the presence of at least two of the following three criteria: hyperandrogenism (either biochemical or clinical), ovulatory dysfunction (oligoovulation or anovulation) and polycystic ovary morphology [2]. PCOS is divided into four main phenotypes (A-D), according to the presence or

* Corresponding author.
** Corresponding author.
E-mail addresses: wdzhou@xmu.edu.cn (W. Zhou), cqhua616@126.com (Q. Chen).

https://doi.org/10.1016/j.heliyon.2024.e36321
Received 5 August 2024; Accepted 13 August 2024
Available online 14 August 2024

absence of these three characteristics [3]. Hyperandrogenism is a common hallmark of PCOS that contributes to clinical phenotypes and fertility dysregulation [1]. Among the four phenotypes (A-D) of PCOS, three phenotypes (A-C) require the hyperandrogenism feature to be present. In addition to infertility, women with PCOS are frequently associated with obesity, insulin resistance, type 2 diabetes mellitus and cardiovascular risk factors. The etiology of this PCOS is still poorly understood, but mounting evidence indicates that PCOS might be a complex multigenic disorder with strong epigenetic and environmental influences [4].

Epigenetic regulation of noncoding RNA (ncRNA) is a research hotspot in the field of reproductive diseases; these include long noncoding RNA (lncRNA), microRNA (miRNA), and PIWI-interacting RNA (piRNA) [5]. LncRNAs are a class of non-coding RNAs (ncRNAs) with a length more than 200 nucleotides that can contribute to transcriptional and post-transcriptional functions [6]. Literatures have showed that changes of lncRNAs in reproductive cumulus cells might be involved in the regulation of oocyte maturation, fertilization, and follicular development [7]. Emerging evidence indicated that aberrant expression pattern change of lncRNA may contribute to the pathogenesis of PCOS and may be potential targets for the diagnosis and treatment of the disease [8,9]. In our previous study, we identified a series of differential expressed lncRNAs from follicular fluid exosmes that may play important roles in the follicular development of PCOS [10]. Currently, although many lncRNAs have been identified to play a crucial role in the pathogenesis of PCOS, the roles and potential mechanisms remain unknown.

Granulosa cells (GCs) are somatic cells arising from the sex cord in the ovary, which are responsible for secreting hormones and supplying nutrients for oocyte growth [11]. As a critical component of the ovary, GCs are also implicated in various ovary-related disorders, such as PCOS and premature ovarian failure (POF) [12]. GCs dysfunction is involved in abnormal follicular development of PCOS. Comparing with women with normal ovarian function, the proliferation levels of GCs in anovulatory PCOS patients are significantly increased [13]. Recently, emerging studies have demonstrated that some lncRNAs affect the function of ovarian GCs and are thereby involved in both physiological conditions and pathological processes [14]. Therefore, lncRNAs may also be considered as potential candidate biomarkers and therapeutic targets in GCs under pathological conditions [14].

On the basis of our previous study [10], this study further demonstrated that lncRNA PKD1P6 expression was down-regulated in GCs of hyperandrogenic PCOS (HA-PCOS) patients and significant negatively correlated with serum testosterone (T) levels. Next, the human ovarian granulose-like tumor cell line KGN was used to investigate the effects of PKD1P6 on proliferation and apoptosis of GCs. The effects of exosomes derived from PKD1P6 overexpression (OE) cells on GCs growth were also examined. Then, the molecular mechanism of PKD1P6/miR-135b axis in regulating the function of GCs was investigated. Finally, the effects of excessive androgen on PKD1P6 expression in vitro and vivo were verified. Altogether, a novel underlying mechanism of PKD1P6 modulating ovarian GCs function in HA-PCOS was revealed.

2. Material and methods

2.1. Patients and clinical sample collection

Participants were recruited at the Reproductive Medicine Center, the First Affiliated Hospital of Xiamen University. The collection and use of all clinical samples in this study were approved by Ethics Committee of the First Affiliated Hospital of Xiamen University, and informed consent was obtained from all participants. All enrolled patients $<$35 years old, had an established diagnosis of primary infertility and would undergo in vitro fertilization (IVF) or intracytoplasmic sperm injection (ICSI) treatment for male factor infertility, tube conditions (the non-PCOS controls, control group) or PCOS (experimental group). Experimental group were eligible for inclusion according to the Rotterdam 2003 criteria for PCOS. Patients with endocrine abnormalities, thyroid disease, ovarian insufficiency, endometriosis and other systematic diseases were excluded.

All participants were treated with ovulation induction through a conventional gonadotrophin-releasing hormone (GnRH) agonist protocol. The oocyte retrieval needle guided by transvaginal ultrasound was used to aspirate the follicular fluid and oocyte from the follicle. Ovarian mural granulosa cells (mGCs) were isolated from follicular fluid samples as previously described [10].The cumulus granulosa cells (cGCs) were separated from the cumulus-oocyte complexes (COCs) and collected as previously described [15]. Centrifuged follicular fluid without visible blood contamination was collected and stored at −80 °C until analyses.

2.2. Cell culture and transfection

The KGN cell line, a steroidogenic human ovarian granulosa-like tumor cell line [16], was obtained from Zhong Qiao Xin Zhou Biotechnology (Shanghai, China). The cells were cultured in Dulbecco's modified Eagle's medium (DMEM)/F12 (BasalMedia, Shanghai, China) containing 10 % fetal bovine serum (FBS) (Gibco, Waltham, MA, USA) and 1 % penicillin-streptomycin (Gibco). For the cell proliferation and viability assay, cells (5×10^3 cells per well) were seeded in 96-well plates and cultured overnight in complete medium. For the cell cycle and apoptosis assays, quantitative real-time polymerase chain reaction and Western blot analysis, cells were seeded in 6-well plates at the optimized density and cultured until reaching 80%–90 %.

The pCDH-CMV-PKD1P6 (NR_123722.1)-EF1-copGFP and pCDH-CMV-MCS-EF1-copGFP (Control) lentiviral plasmid were purchased from GENERAL BIOL (Anhui, China). Then stable KGN cell lines with PKD1P6 overexpression (PKD1P6 OE) or control vector were constructed. For gain-of-function experiments of miR-135b-5p, KGN cells were transfected with miR-135b-5p mimic or negative control (NC) (RiboBio, Guangzhou, China) by using Lipofectamine RNAiMAX (Thermo Fisher) according to the manufacturer's instructions.

2.3. Cell proliferation assay

The cell counting kit-8 (CCK-8) assay was used to detect cell viability. After each indicated time of culture in 96-well plates, cells were incubated for another 2 h in fresh medium containing CCK-8 reagent (Solarbio). The optical density (OD) at 450 nm was assessed with a microplate reader. 5-ethynyl-2′-deoxyuridine (EdU) assays were performed using BeyoClick™ EdU-594 Kit or BeyoClick™ EdU-488 Kit (Beyotime Institute of Biotechnology, Shanghai, China) according to the manufacturer's protocol. Cell nucleus were stained with Hoechst 33342 or DAPI and image were taken by using Nikon Eclipse Ci fluorescent microscope (Tokyo, Japan).

2.4. Flow cytometry analysis

For cell cycle analysis, cells were collected and resuspended in PBS. Then, cells were fixed in cold ethanol (70 %) at 4 °C overnight. After washed with PBS, cells were stained with RNase and propidium iodide (PI) reagent in the darkness. For cell apoptosis analysis, the assay was performed using Annexin V-Alexa Fluor 647/PI Apoptosis Detection Kit (Biotechnology, Shanghai, China) or PE Annexin V Apoptosis Detection Kit I (BD Biosciences, San Jose, CA, USA) according to the manufacturer's instructions. After finishing the dyeing process, cell suspension was analyzed using CytExpert flow cytometry (Beckman, California, USA) with manufacturer recommended machine setting.

2.5. Reverse transcription quantitative real-time PCR (RT-qPCR)

Total RNA was extracted by using TRIzol Reagent (Invitrogen, Waltham, MA, USA) following the manufacturer's directions. Reverse transcription (RT) PCR was performed with the SuperScript™ Reverse Transcriptase (Invitrogen) to synthesize complementary DNA (cDNA). Quantitative real-time PCR was applied on LightCycler ® 480 Real-Time PCR System (Roche, Basel, Switzerland) with SYBR® Green Premix Pro Taq HS qPCR Kit (Accurate Biology, Hunan, China). β-actin or GAPDH was used as an internal control for PKD1P6, PCNA, cyclin D1, p21, p27, Bax, caspase-3 and caspase-9, and U6 for miR-135b-5p. Relative expression levels of these indicators were calculated by the $2^{-\Delta\Delta Ct}$ method. The sequences of the primers are presented in Supplementary Table S1.

2.6. Western blot analysis

Cells were lysed on ice in radioimmunoprecipitation assay lysis buffer (RIPA; Thermo Fisher Scientific, MA, USA) containing protease/phosphatase inhibitor mixture (Roche) for protein extraction. Protein samples were separated via SDS-PAGE followed by transfer onto polyvinylidene difluoride (PVDF) membrane (Millipore, MA, USA). The protein-contained membranes were blocked in 5 % skim milk at room temperature for an hour, and then incubated with primary antibodies overnight at 4 °C. After washing, the membranes were incubated with the corresponding secondary antibodies for 1 h at room temperature. Then Chemiluminescence Image Capture System (Thermo Fisher) was performed for protein band visualization. The antibodies used in this study are Supplementary Table S2.

2.7. Isolation and characterization of exosome

Exosomes from cell culture supernatants were isolated and purified by ultracentrifugation according to previous protocol [17]. Briefly, cell culture medium was centrifuged at 500 g for 5min, and the supernatants were centrifuged again at 2000 g for 30 min to remove cell debris. Then the supernatants were centrifuged at 10000 g for 60 min and passed through 0.22 μm membrane filter. After transferred to new polycarbonate tubes, the supernatants were centrifuged at 120000 g for 70 min. All the centrifugations were carried out at 4 °C. Isolated exosomes were resuspended in PBS and store at −80 °C for further use. The quantity of isolated exosomes was determined by BCA protein assay (TaKaRa, Dalian, China). The morphology of isolated exosomes was visualized by using transmission electron microscopy (TEM) (Hitachi HT7700, Japan). The distribution of exosome sizes was measured by NanoSight NS300 (Malvern, UK). The markers (TSG101, CD9 and CD81) of exosome were detected by Western blot.

2.8. Exosome uptake assay

Exosomes were labeling with a fluorescence dye PKH67 (PKH67 Green Fluorescent Cell Linker Midi Kit, Sigma, USA) to make sure that they could be took up by recipient cells. First, PKH67 was mingled with exosomes and incubated for 5 min at room temperature. Then 1 % BSA was added to terminate the dyeing. Next, the labeled exosomes were collected by centrifugation (120000 g, 70 min) and resuspended in PBS, followed by adding into 24-well plate containing KGN cells for different incubation time (8 h, 16 h, 24 h) at 37 °C in 5 % CO_2 cell culture incubator. After the steps of fixing, cleaning and membrane rupturing, the cells were stained with DAPI to label nuclei. Finally, fluorescence images were collected using a Nikon Eclipse TI-SR fluorescence microscope (Tokyo, Japan).

2.9. Fluorescence in-situ hybridization (FISH)

FISH probe design and labeling specificity identification were done by RiboBio (Guangzhou, China). To fix the mGCs, 4 % paraformaldehyde (PFA; Solarbio, Beijing, China) were added to prepared mGCs climbing slices and incubated at room temperature for 20

min. The slices were then washed twice with PBS and digested in 20 μg/ml proteinase K (Servicebio, Wuhan, China) and repeated washing process. The Cy3-labeled PKD1P6 FISH probe or U6 and 18S FISH probes as internal controls were then added into mGCs and incubated overnight at 37 °C using a biochemical incubator. After hybridization, slides were then washed twice with washing buffer and stained the cell nucleus using 4′,6-diamidino-2-phenylindole (DAPI) (Servicebio) for 5 min before imaging. Fluorescence images of DAPI-stained samples mounted on coverslips were exanimated and collected using a Nikon Eclipse TI-SR fluorescence microscope (Tokyo, Japan).

2.10. Dual-luciferase reporter assay

The predicted binding site of miR-135b-5p to PKD1P6 was amplified and inserted into the psiCHEK-2 Vector between *Xho*I and *Not*I restriction sites. The reporter vector psiCHEK-2-PKD1P6-wt contains the predictive binding site of miR-135b-5p. The reporter vector psiCHEK-2-PKD1P6-mut contains point mutations of the miR-135b-5p seed binding site. HEK-293T cells were cultured and co-transfected with psiCHEK-2-PKD1P6-wt or psiCHEK-2-PKD1P6-mut vector, miR-135b-5p mimic and miR-NC using Lipofectamine 3000 (Invitrogen). The Firefly and Renilla luciferase activities were measured using microplate reader. The Renilla luciferase activities were normalized to Firefly luciferase activities.

2.11. Treatment of KGN cells by dihydrotestosterone (DHT)

KGN cells were plated in 6-well plates at 2×10^5 per well. When the cell density reached 60–70 %, serum was starved for 4 h, followed by DHT (Solarbio) stimulation. For the dose-response experiments, the cells were treated by DHT for 24 h with different doses (0, 5, 10, 25, 50 nM). For the time-response experiments, the cells were treated by DHT (50 nM) for different time (0, 12, 24, 48, 72 h).

2.12. PCOS rat model

Female Sprague-Dawley (SD) rats used in this study were purchased and carefully fed under specific pathogen-free conditions in a temperature-controlled room (24 ± 1 °C) with 12 h light/12 h dark cycle and *ad libitum* access to food and water by the Animal Experimental Center of Xiamen University. SD rats (about six weeks) were randomly assigned into the PCOS model group (PCOS) and the control group (sham). The PCOS model group was induced by 1 mg/kg letrozole dissolved in 1 % carboxymethylcellulose (CMC) solution once daily p.o. for 21 days and the sham received 10 g/L CMC once daily p.o. only for an equivalent length of duration. For morphological evaluation, fixed ovaries were paraffin embedded and sectioned at a thickness of 4 μm. Then paraffin section stained with hematoxylin-eosin (HE) stain kit according to the manufacturer's protocol. The hormone levels were determined by the enzyme

Table 1
Basic clinical features of women with and without PCOS.

	Name	Group	n	Mean	Std. Deviation	F test to compare variances		T-test for Equality of Means		
						F	Sig.	Sig.(2-tailed)	95 % Confidence Interval	
									Lower	Upper
Anthropometric variables	Age (years)	Control	26	29.50	3.38	1.186	0.7036	0.2909	−2.953	0.906
		PCOS	21	28.48	3.11					
	Infertility (years)	Control	26	2.96	2.50	1.546	0.3235	0.4498	−0.845	1.874
		PCOS	21	3.48	2.02					
	BMI (kg/m2)	Control	26	22.04	3.19	3.224	0.0064	0.5003	−1.763	3.559
		PCOS	21	22.94	5.73					
Serum hormone levels	**AMH** (ng/mL)	Control	26	4.92	2.66	3.122	0.008	**0.0008*****	1.702	6.078
		PCOS	21	8.80	4.69					
	E2 (pg/mL)	Control	26	45.85	19.19	2.372	0.0423	0.2690	−6.392	22.380
		PCOS	21	53.85	29.55					
	T (ng/dL)	Control	26	30.95	15.21	1.182	0.6840	**0.0000******	23.39	42.09
		PCOS	21	63.69	16.54					
	FSH (IU/L)	Control	26	7.051	2.39	2.636	0.0303	0.6773	−1.453	0.9529
		PCOS	21	6.801	1.47					
	LH (IU/L)	Control	26	4.021	2.21	3.172	0.0071	**0.0000******	2.321	5.990
		PCOS	21	8.177	3.94					
	P (ng/mL)	Control	26	0.5904	0.28	1.093	0.8227	0.6736	−0.1343	0.2059
		PCOS	21	0.6262	0.29					
	PRL (ng/mL)	Control	26	15.42	5.82	1.874	0.1554	0.1356	−5.371	0.7515
		PCOS	21	13.11	4.25					
	FPG (mmol/L)	Control	26	5.108	0.32	1.550	0.3205	0.5543	−0.2250	0.1203
		PCOS	21	5.056	0.26					

BMI: body mass index; AMH: anti-Müllerian hormone; E2: estradiol; T: testosterone; FSH: follicular stimulating hormone; LH: luteinizing hormone; P: Progesterone; PRL: prolactin; FPG: fasting plasma glucose. *significant difference between Control group and PCOS group.

linked immunosorbent assay (ELISA) method according to the manufacturer' s instruction. Animal studies in this paper were approved by the Ethics Committee on Animal Experiments at Xiamen University (ethical protocol number: XMULAC20180078). All animal experiments were performed in accordance with the guidelines of the Animal Experimental Center of Xiamen University.

2.13. Statistical analysis

Data were analyzed using GraphPad Prism 9.0 software (GraphPad Software, Inc., San Diego, CA, USA). Data were presented as means ± SD. Statistical differences were determined by an unpaired parametric *t*-test or by one-way ANOVA parametric test. The correlation analyses were used to examine the association between PKD1P6 expression and the levels of relevant clinical characteristics. P value < 0.05 was considered statistically significant.

3. Results

3.1. Clinical characteristics of patients

A total of 47 patients undergoing IVF/ICSI treatment were enrolled in this study, including 21 experimental group patients with PCOS and 26 control group patients with normal ovarian function. The main characteristics of these patients were shown in Table 1. It was shown that the two groups were similar in anthropometric variables, such as age, body mass index (BMI) and infertile years. Testosterone (T), luteinizing hormone (LH) and anti-Müllerian hormone (AMH) levels in serum were significantly higher in the PCOS group compared with the control group, while no difference was observed in follicular stimulating hormone (FSH), fasting plasma glucose (FPG), estradiol (E2) and progesterone (P) and prolactin (PRL). Overall, the experimental group patients were consistent with the typical hormone features of hyperandrogenic PCOS (HA-PCOS).

3.2. Characteristics of PKD1P6 in ovarian GCs of HA-PCOS

Our previous study found that the level of lncRNA PKD1P6 (NR_123722.1) was obviously decreased in follicular fluid exosomes of PCOS patients (Fig. 1A). In this study, the expression of PKD1P6 was further verified in cGCs of HA-PCOS patients (n = 21) and non-PCOS controls (n = 26). As illustrated in Fig. 1B, the expression of PKD1P6 was significantly decreased in cGCs of PCOS patients

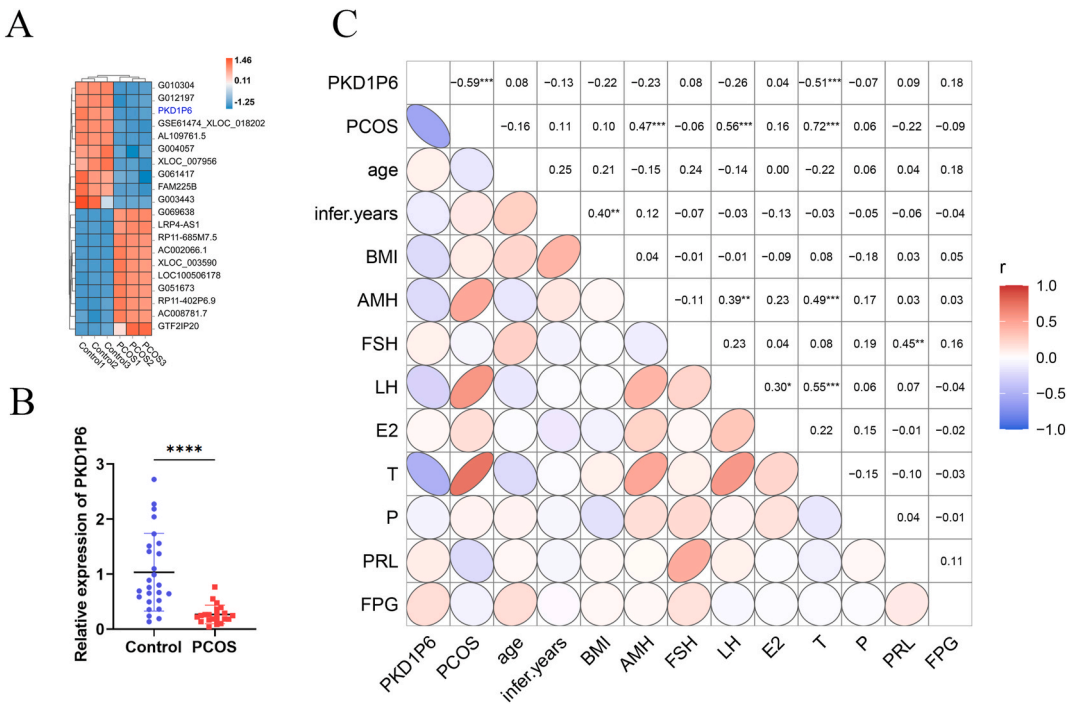

Fig. 1. Expression pattern of PKD1P6 in granulosa cells (GCs) of PCOS. (A) Heatmap of differentially expressed exosomal lncRNAs in PCOS and the control follicular fluid (top20). (B) The expression of PKD1P6 in cumulus granulosa cells (cGCs) of 21 PCOS patients and 26 non-PCOS controls was determined by RT-qPCR. β-actin was used for normalization. ****$P < 0.0001$. (C) The correlation between PKD1P6 expression in cGCs and clinical parameters in patients was analyzed using Pearson's correlation analysis. ***$P < 0.001$. BMI: body mass index; AMH: anti-Müllerian hormone; E2: estradiol; T: testosterone; FSH: follicular stimulating hormone; LH: luteinizing hormone; P: Progesterone; PRL: prolactin; FPG: fasting plasma glucose.

compared with in non-PCOS controls. In addition, the correlation analysis between PKD1P6 level in cGCs and clinical parameters of patients was carried out. The results showed that the expression of PKD1P6 in cGCs was significant negatively correlated with PCOS ($r = -0.59$, $P = 0.00015$) and serum testosterone (T) level ($r = -0.51$, $P = 0.0003$). Besides PCOS and T level, there is no significant correlation between PKD1P6 level and other clinical parameters (Fig. 1C).

Considering that the localization of lncRNA is a crucial process for cellular function, the subcellular localization of PKD1P6 in primary cultured human mGCs and human ovarian granulosa cell line KGN was analyzed by FISH. The results revealed that PKD1P6 was mainly distributed in the cytoplasm of mGCs from HA-PCOS patients and non-PCOS controls. Similar result was also observed in KGN cell line (Fig. S1).

3.3. Effects of PKD1P6 on the functions of GCs

To investigate the effects of PKD1P6 on the biological function of ovarian GCs, lentivirus-mediated PKD1P6 overexpression (PKD1P6 OE) KGN cell line was constructed (Fig. 2A). CCK-8 and EdU assays consistently showed that PKD1P6 overexpression significantly attenuated cell viability and DNA synthesis capacity of KGN cells compared with control (Fig. 2B–C). In addition, the cell cycle distribution was analyzed by means of flow cytometry. Comparing with the control group, the percentage of G0/G1 phase in PKD1P6 OE cells was significantly increased and the S and G2/M phases were significantly decreased (Fig. 2D). Moreover, the expressions of proliferation-related genes such as PCNA, Cyclin D1, p27 and p21 were determined by RT-qPCR and Western blot. As shown in Fig. 2E–G, PKD1P6 overexpression significantly inhibited expressions of the key cycle commanders PCNA and cyclin D1. In contrast, PKD1P6 overexpression significantly promoted the expressions of cyclin-dependent kinases (CDKs) inhibitors p27 and p21.

In addition, to assess the role of PKD1P6 in ovarian granulosa cell apoptosis, Annexin V/PI staining was employed. As shown in Fig. 3A, PKD1P6 overexpression significantly promoted the apoptotic rate of KGN cells. Then, the expressions of apoptosis-associated genes such as caspase-3, caspase-9 and Bax were detected by RT-qPCR and Western blot. The results showed that PKD1P6 overexpression significantly increased the expressions of three apoptosis promoters (caspase-3, caspase-9 and Bax) (Fig. 3B–C).

3.4. Effects of exosomes derived from PKD1P6-overexpression cells on the growth of GCs

Our previous study indicated that a number of lncRNAs including PKD1P6 in follicular fluid exosmes might be involved in the pathogenesis of PCOS [10]. To examine whether exosome involved in mediating PKD1P6 to regulate the growth of GCs, exosomes derived from PKD1P6-overexpression cells were co-cultured with KGN cells. The observation of fluorescence confocal microscopy revealed that exosomes derived from PKD1P6 OE or empty control cells could be taken up by KGN cells (Fig. 4). The results of CCK-8 and EdU assays showed that exosomes from PKD1P6-overexpression cells significantly inhibited the cell viability and DNA synthesis capacity of KGN cells (Fig. 5A–B). Consistently, after co-culturing with PKD1P6 OE-derived exosomes, the proportion of KGN cells in G0/G1 phase was significantly increased and the proportion of KGN cells in S and G2/M phases was significantly decreased (Fig. 5C).

3.5. PKD1P6 directly targets miR-135b-5p

To further explore whether PKD1P6 acts as a competing endogenous RNA (ceRNA) to exert its regulatory effects on GCs growth, bioinformatic analysis was used to screen the potential target of PKD1P6. Through combining the predicted ceRNAs of PKD1P6 (from Starbase) with the up-regulated miRNAs in GCs of PCOS patients ($P < 0.05$, Fold Change >2) (data from GSE72274), miR-135b-5p was found to have a complementary binding sequence of PKD1P6 (Fig. 6A–B). To confirm the expected binds, dual-luciferase reporter assays were exploited. Both wild- and mutant-type PKD1P6 luciferase reporter plasmids were produced for the dual-luciferase reporter experiment, and the plasmids were co-transfected with miR-135b-5p mimic or miR-NC in HEK 293T cells. RT-qPCR analysis showed that the expression of miR-135b-5p was significantly increased when PKD1P6-wt (wild-type plasmids) or PKD1P6-mut (mutant-type plasmids) co-transfected with miR-135b-5p mimic ($P < 0.0001$) (Fig. 6C). Luciferase reporter assays showed that when co-transfected of PKD1P6-wt with miR-135b-5p mimic, the luciferase activity was significantly reduced ($P < 0.01$). However, there was no significant change in luciferase activity after co-transfection of PKD1P6-mut with miR-135b-5p mimic ($P > 0.05$) (Fig. 6D). In addition, overexpression of PKD1P6 in KGN cells could lead to significant downregulation of miR-135b-5p expression level ($P < 0.01$) (Fig. 6E). Collectively, these data suggested that PKD1P6 could directly bind to miR-135b-5p to downregulate its expression.

3.6. miR-135b-5p promotes cell survival, proliferation and inhibits cell apoptosis of GCs

miR-135b-5p is a downstream target of PKD1P6; therefore, this study further evaluated the effects of miR-135b-5p on the growth of GCs. KGN cells were transfected with miR-135b-5p mimic, and then miR-135b-5p levels were analyzed by RT-qPCR. As expected, transfection with miR-135b-5p mimic markedly increased miR-135b-5p levels (Fig. 7A). Cell viability, DNA synthesis capacity, cell cycle distribution and cell apoptosis were assessed by CCK-8 assay, EdU assay and flow cytometry, respectively. The results showed that up-regulation of miR-135b-5p significantly promoted cell viability and DNA synthesis capacity (Fig. 7B–C). miR-135b-5p overexpression significantly decreased the proportion of KGN cells in G0/G1 phase and increased the proportion of cells in the S phase. There was no significant difference in the proportion of cells in the G2/M phases (Fig. 7D). Additionally, the cell apoptosis analysis revealed that miR-135b-5p overexpression significantly inhibited the apoptotic rate compared with the miR-NC group ($P < 0.001$) (Fig. 7E).

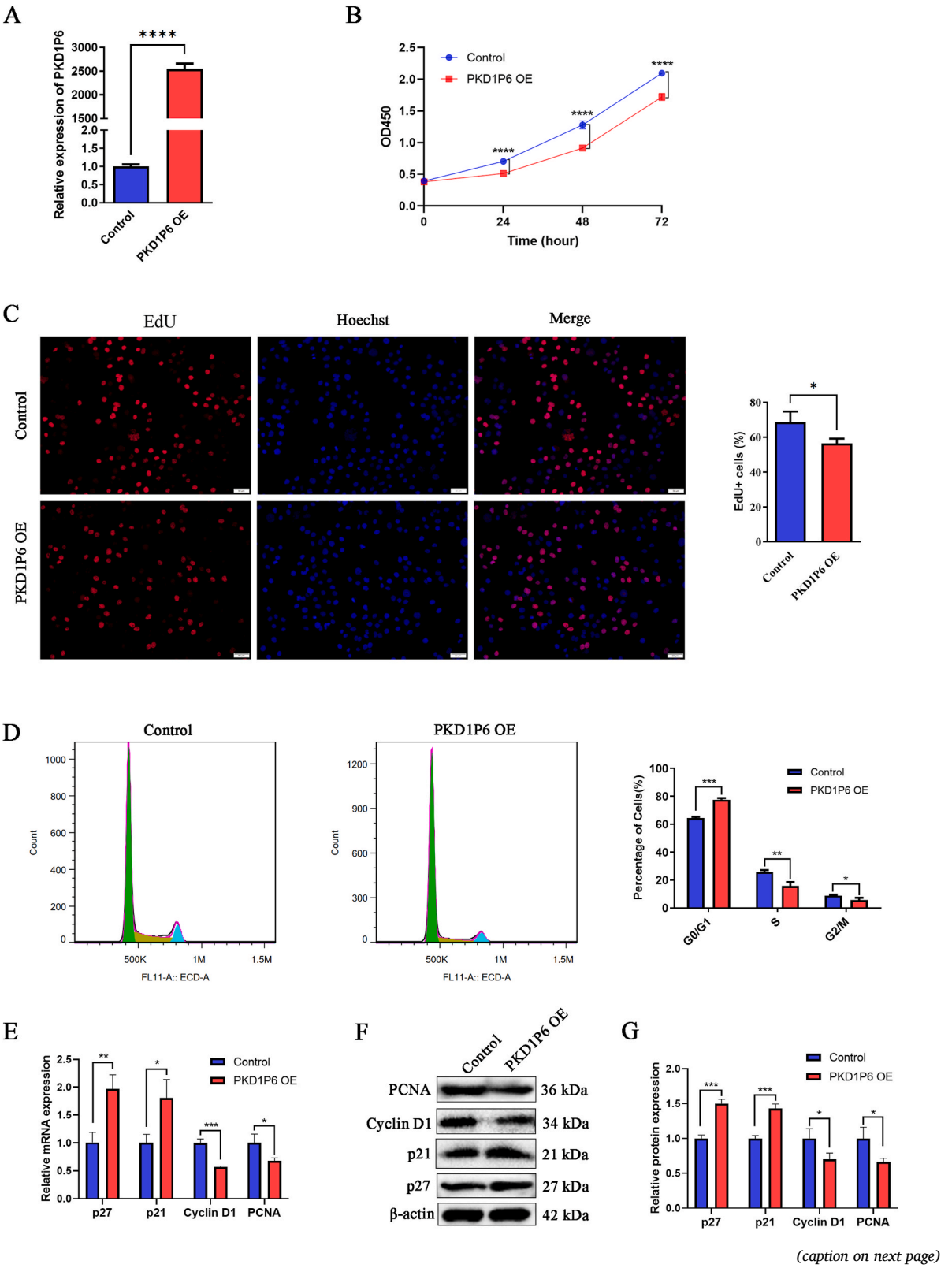

(caption on next page)

Fig. 2. Overexpression of PKD1P6 inhibits the proliferation of GCs. (A) Efficiency of PKD1P6 expression in PKD1P6 overexpressed (OE) KGN cells was verified by RT-qPCR. (B) The evaluation of cell viability via CCK-8 assays. (C) DNA synthesis capacity was examined by EdU assays. Scale bar = 50 μm. (D) Cell cycle distribution was analyzed by flow cytometry. (E) The mRNA expression of proliferation-related regulators was assessed by RT-qPCR. (F–G) The protein expression of proliferation-related regulators was detected by Western blot. β-actin was used as an internal control. $^{*}P < 0.05$, $^{**}P < 0.01$, $^{***}P < 0.001$, $^{****}P < 0.0001$.

3.7. Effects of PKD1P6/miR-135b-5p axis on MAPK signaling pathway

The mitogen-activated protein kinase (MAPK) signaling pathway has been implicated in the regulation of cell proliferation and cell apoptosis. To further investigate the regulatory mechanism of PKD1P6/miR-135b-5p axis in the growth of granulosa cells, effects of PKD1P6 and miR-135b-5p overexpression on activities of p38, JNK and ERK1/2 were assessed by Western blot. As depicted in Fig. 8A–D, PKD1P6 overexpression significantly suppressed ERK1/2 phosphorylation in KGN cells. However, there was no significant change in the levels of phosphorylated JNK and p38 when PKD1P6 was overexpressed in KGN cells. In contrast, up-regulation of miR-135b-5p significantly increased phosphorylation level of ERK1/2. Similar to PKD1P6 overexpression, there was no significant difference in the levels of phosphorylated JNK and p38 when miR-135b-5p was up-regulated in KGN cells (Fig. 8E–H).

3.8. Effects of excessive androgen on PKD1P6 expression in vitro and vivo

To further verify the expressions of PKD1P6 and miR-135b-5p in HA-PCOS, we treated KGN cells with DHT, the non-aromatizable androgen, to simulate the pathophysiologic status of HA-PCOS. The RT-qPCR analysis showed that PKD1P6 was down-regulated in DHT-induced KGN cells (Fig. 9A–B). Conversely, the expression of miR-135b-5p was increased after treatment with DHT for different doses and times (Fig. 9C–D).

Furthermore, the expressions of PKD1P6 and miR-135b-5p were also assessed in letrozole-induced PCOS rat model. As depicted in Fig. 9E–F, the PCOS rats manifested the major symptoms of PCOS in humans, including typical polycystic ovarian (PCO) morphology and excessive androgen. The results of RT-qPCR showed that PKD1P6 level was significantly down-regulated in ovaries of PCOS rats compared with the control rats (Fig. 9G). Conversely, the expression of miR-135b-5p was significantly elevated in ovaries of PCOS rats (Fig. 9H).

4. Discussion

In this study, we provided evidence for the first time that lncRNA PKD1P6 functions as an important regulator in ovarian GCs growth during follicular development of PCOS. Specifically, we initially found that PKD1P6 was remarkably down-regulated in ovarian GCs of HA-PCOS and negatively correlated with serum testosterone levels. Overexpression of PKD1P6 contributed to the function change of GCs, including attenuated cell proliferative capacity, arrested cell cycle progression and promoted cell apoptosis. Exosomes derived from PKD1P6-overexpression cells exerted similar effects to PKD1P6 overexpression on the function of GCs. Mechanistically, PKD1P6 was found to directly target miR-135b-5p and down-regulate miR-135b-5p expression. PKD1P6/miR-135b-5p axis was involved in modulating the function of GCs partly via regulating the activity of ERK1/2 signaling pathway. In addition, excessive androgen was showed to inhibit PKD1P6 expression while increase miR-135b-5p expression of PCOS models in vitro and vivo.

LncRNAs are crucial for numerous cellular processes, including cell proliferation, apoptosis, differentiation, and metabolism. Recently, there is growing evidence that dysregulated lncRNAs play important roles in the growth of GCs and the pathogenesis of PCOS [14,18]. In this study, we found that lncRNA PKD1P6 was abnormally decreased in cGCs of HA-PCOS patients and was negatively correlated with serum testosterone level. Moreover, down-regulated PKD1P6 was also observed in DHT-induced KGN cells and letrozole-induced PCOS rat model. As we known, excessive androgen production by the ovaries is a key feature of HA-PCOS [3]. Therefore, it is indicated that low expression of PKD1P6 in HA-PCOS might be involved in the development of this disease.

Ovarian granulosa cells (GCs) are somatic cells surrounding oocytes within follicles and are essential for folliculogenesis [14]. Previous studies have shown that the uncontrolled growth of GCs contributed to aberrant folliculogenesis of PCOS [19,20]. To investigate the roles of PKD1P6 in the growth of GCs, in this study, PKD1P6 was overexpressed in a human ovarian granulosa cell line KGN. It was found that PKD1P6 overexpression significantly inhibited cell growth and promoted cell apoptosis. Combining with the low expression of PKD1P6 in HA-PCOS, it is suggested that PKD1P6 is crucial for the homeostasis of GCs function in HA-PCOS.

It is known that dysregulation of cell cycle is a main cause of abnormal cell proliferation. Proliferating cell nuclear antigen (PCNA) is a protein which is involved in cell cycle regulation and DNA replication [21]. Cyclin D1 plays a critical role in promoting the G1-S transition of the cell cycle in many different cell types [22]. Cyclin dependent kinase (CDK) inhibitor p21 and p27 are key factors that inhibit the progression of the cell cycle [23,24]. In this study, we found that PKD1P6 overexpression caused cell cycle arrest at G0/G1 phase in KGN cells. Moreover, up-regulation of PKD16 significantly inhibited the expressions of PCNA and cyclin D1, but promoted the expressions of p27 and p21. These findings suggest that PKD1P6 affect cell cycle progression of GCs by regulating the expression of these proliferation-related regulators. In addition, activated caspase-3, which is functionally required for the execution of cell death, was reported to be significantly decreased in GCs of anovulatory PCOS follicles in comparison with normal ovulatory follicles [20]. In the present study, our results revealed that PKD1P6 overexpression significantly promoted the expressions of apoptosis regulators such as caspase-3, caspase-9 and Bax. These evidences indicated that lower level of PKD1P6 in GCs of HA-PCOS might lead to apoptosis

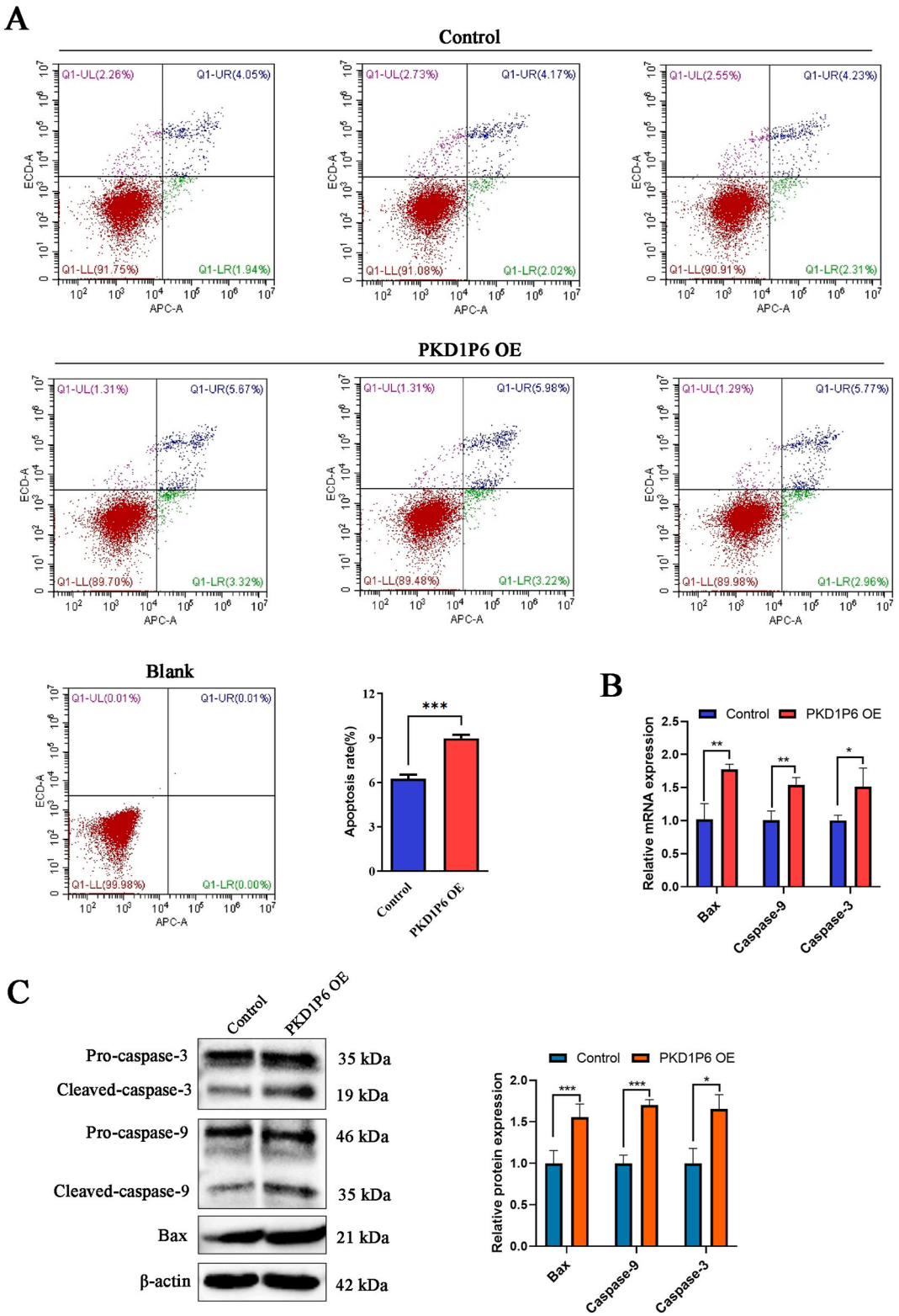

Fig. 3. Overexpression of PKD1P6 promotes apoptosis of GCs. (A) Flow cytometry were performed to analyze the apoptotic rate in PKD1P6 overexpressed (OE) KGN cells. (B) The mRNA expression of apoptosis-associated genes was determined by RT-qPCR. (C) The protein expression of apoptosis-associated proteins was determined by Western blot. β-actin was used as an internal control. $^{*}P < 0.05$, $^{**}P < 0.01$, $^{***}P < 0.001$.

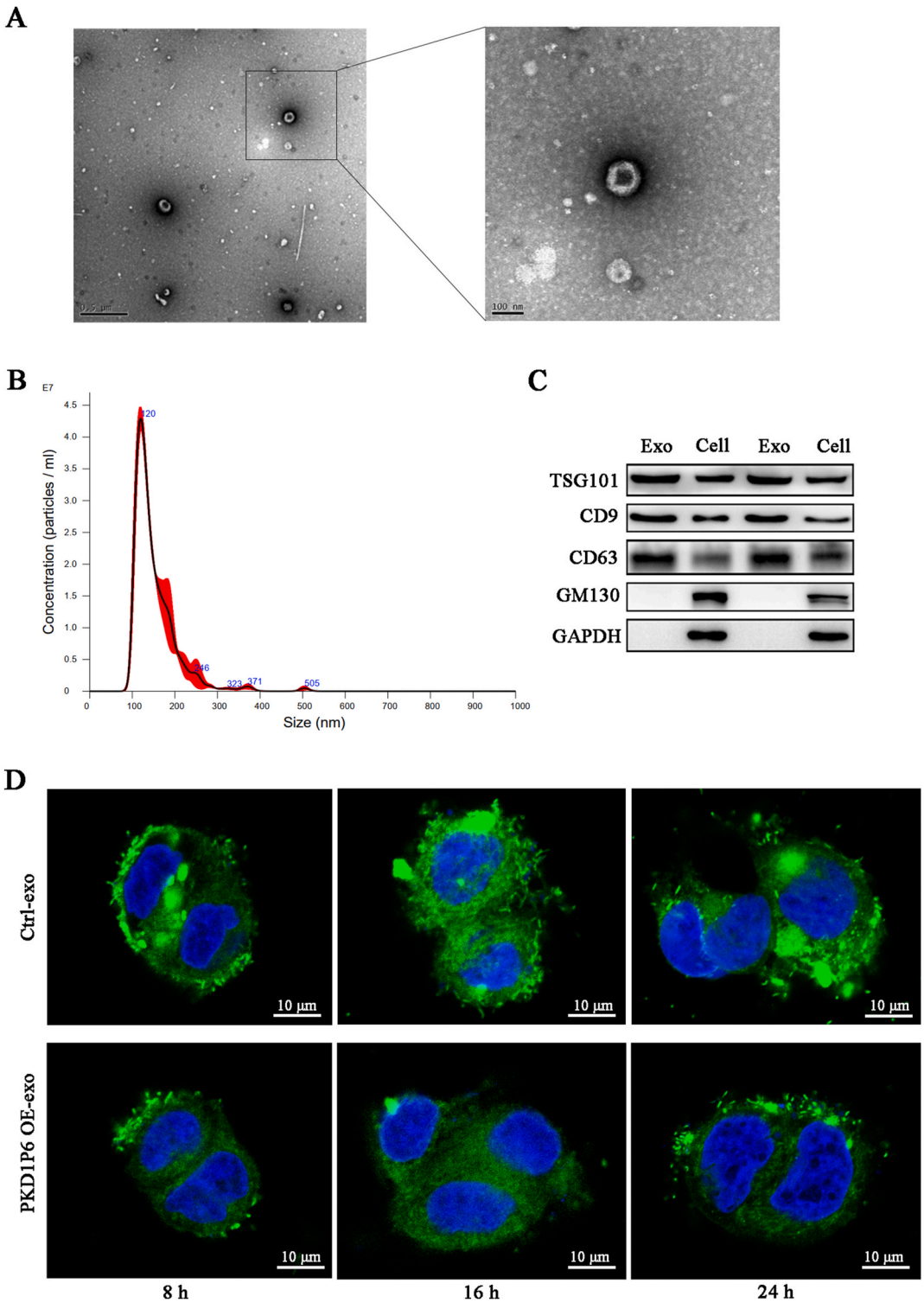

Fig. 4. Exosome (Exo) characterization and uptake assays. (A) Representative transmission electron microscopy (TEM) images of exosomes isolated from KGN cell culture supernatants. Scale bar = 100 nm. (B) Nanoparticle tracking analysis of the size distribution and concentration of exosomes. (C) The protein expression of exosome markers was analyzed by Western blot. (D) Exosomes derived from PKD1P6 overexpressed (OE) cells were co-cultured with KGN cells. The subcellular location of exosomes taken up by KGN cells were observed by fluorescence confocal microscopy. Exosomes were labeled with PKH67 (green). Nuclei were stained with DAPI (blue). Scale bar = 10 μm.

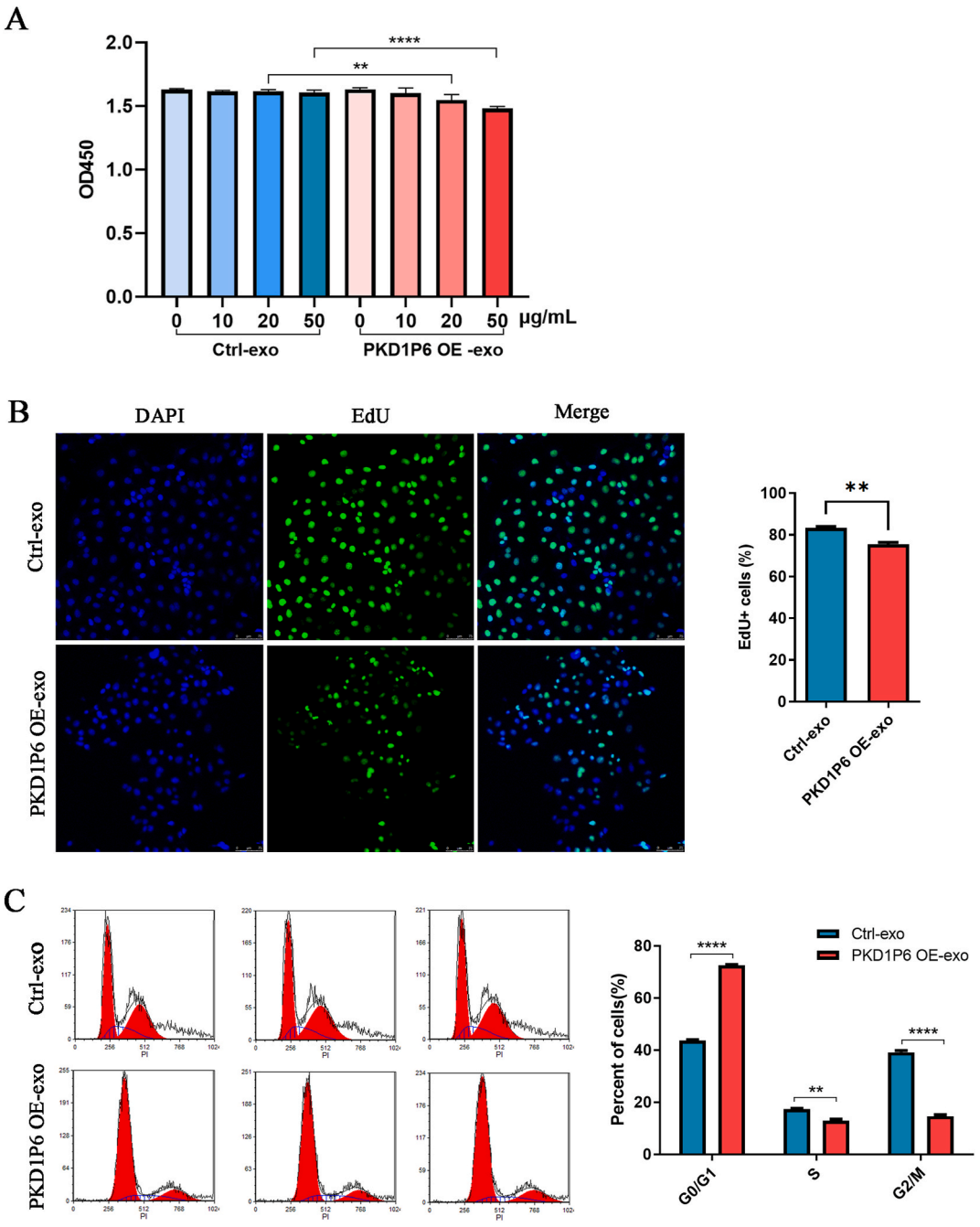

Fig. 5. Exosomes derived from PKD1P6 overexpressed (OE) cells promote the proliferation of GCs. (A) Cell viability was determined by CCK-8 assays. (B) DNA synthesis capacity was examined by EdU assays. Scale bar = 75 μm. (C) Cell cycle distribution was analyzed by flow cytometry. $^{**}P < 0.01$, $^{****}P < 0.0001$.

resistance by modulating the expressions of apoptosis-associated genes, and thereby accelerated the proliferation of GCs.

The function of lncRNA is directly associated with their location. LncRNAs which are expressed in the cytoplasm participate in post-translational modification, protein localization procedures as well as the stability and translation of mRNA [25]. It is well known that competitive endogenous RNA (ceRNA) is an important regulatory mechanism of lncRNA highly expressed in the cytoplasm. LncRNA can competitively binding its common miRNAs by specific binding sites, thereby regulating the expression of its downstream target genes [26]. In this study, it was found that PKD1P6 was mainly located in the cytoplasm of GCs, suggesting that PKD1P6 may act on its roles though ceRNA mechanism. Furthermore, results of dual-luciferase reporter assays and cell function assays proved that PKD1P6 acted as a ceRNA of miR-135b-5p to regulate the growth of GCs. In addition, up-regulation of miR-135b-5p promoted cell growth and

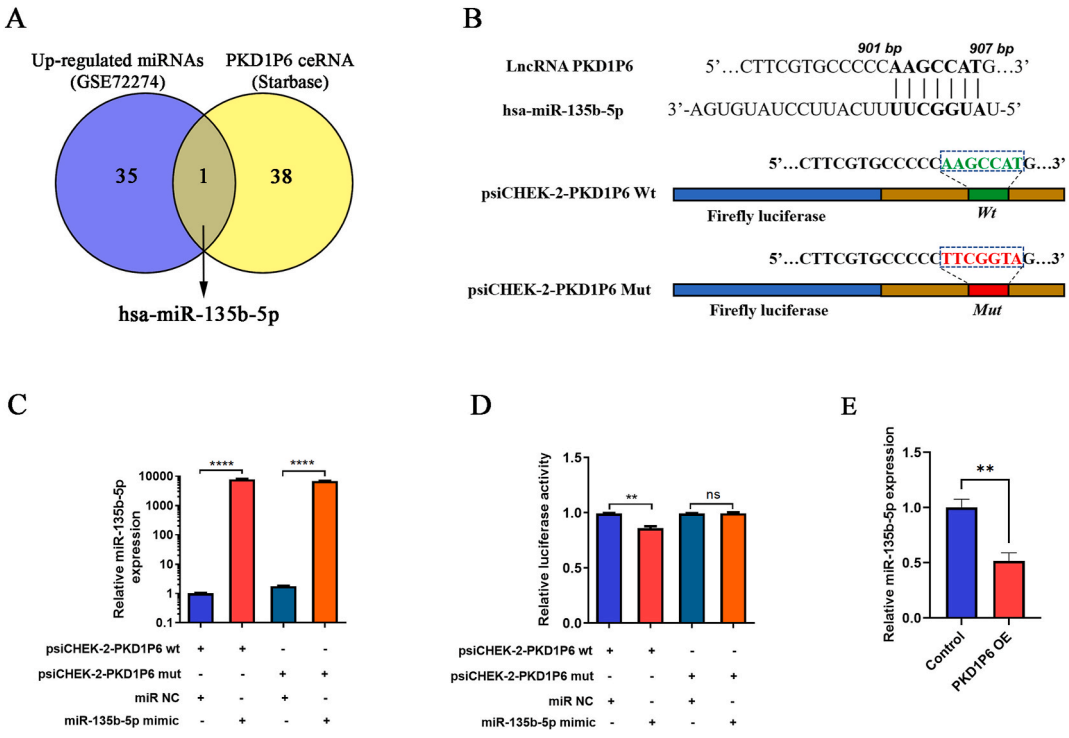

Fig. 6. PKD1P6 acts as a ceRNA for miR-135b-5p. (A) Bioinformatics analysis and Venn diagram analysis showing miR-135b-5p as a potential miRNA binding to PKD1P6. (B) Schematic diagram showing the predicted miR-135b-5p binding sites with PKD1P6. The sequences of wild-type (*Wt*) and mutant (*mut*) PKD1P6 were also listed. (C) The expression of miR-135b-5p was detected in HEK293T cells by RT-qPCR. (D) Dual-luciferase reporter assays were performed to measure the luciferase activity in HEK293T cells. (E) Relative miR-135b-5p expression level was determined in PKD1P6 overexpressed (OE) KGN cells by RT-qPCR. U6 was used for normalization. $^{**}P < 0.01$, $^{****}P < 0.0001$. ns: no significant difference.

inhibited cell apoptosis in GCs. These findings suggested that PKD1P6 could suppress GCs cell proliferation and promoted the cell apoptosis though targeting miR-135b-5p and down-regulating its expression.

Recently, various exosomal ncRNAs have been reported to express abnormally in PCOS patients and play key roles in the development of the disease. A recent study discovered that miR-424-5p derived from follicular fluid exosome of PCOS could inhibit GCs proliferation and induce GCs senescence by targeting CDCA4 expression [27]. Moreover, another research showed that follicular fluid-derived exosomal miR-18b-5p could regulate PTEN-mediated PI3K/Akt/mTOR signaling pathway to suppress the progression of PCOS [28]. In addition, our previous study identified a number of differential expressed lncRNAs including PKD1P6 from follicular fluid exosmes of PCOS patients which were related to the pathogenesis of PCOS [10]. In this study, it was found that exosomes derived from PKD1P6-overexpression cells could suppress the growth of GCs, which exerted similar effects to PKD1P6 overexpression on the function of GCs. These findings suggested that exosomes were involved in mediating PKD1P6 to regulate the growth of GCs in the folliculogenesis of PCOS.

Extracellular signal-regulated protein kinases 1 and 2 (ERK1/2), which are also referred to as mitogen-activated protein kinase 3 and 1 (MAPK3/1), are members of the mitogen-activated protein kinase super family that can mediate cell proliferation and apoptosis [29]. Especially, GCs from PCOS patients exhibited increased phosphorylation of ERK compared with those of control individuals [30]. In addition, increased ERK1/2 and phospho-ERK1/2 (p-ERK1/2) were also observed in ovarian tissues of PCOS model rats [31]. In this study, our results showed that overexpression of PKD1P6 significantly restrained the phosphorylation of ERK1/2, and up-regulation of miR-135b-5p significantly enhanced the phosphorylation of ERK1/2 in KGN cells. Overall, these findings indicated that imbalance of PKD1P6/miR-135b-5p axis in PCOS might trigger dysfunction of GCs proliferation and apoptosis partially through regulating the ERK1/2 signaling pathway.

5. Conclusions

We comprehensively investigated the clinical characteristics, functional roles, and molecular mechanisms of PKD1P6 in HA-PCOS. Our results demonstrated that PKD1P6 was remarkably down-regulated in GCs of HA-PCOS. PKD1P6 expression level was negatively correlated with serum testosterone levels in HA-PCOS patients. Excessive androgen levels might be an important cause of PKD1P6 down-regulation in HA-PCOS. The dysregulation of PKD1P6/miR-135b-5p axis could result in abnormal cell proliferation and apoptosis of GCs partially though activating ERK1/2 signaling, and then led to abnormal folliculogenesis of PCOS (Fig. 10). This study reveals that PKD1P6 plays a crucial part in the development of PCOS and highlighted its value as a novel molecular target for the

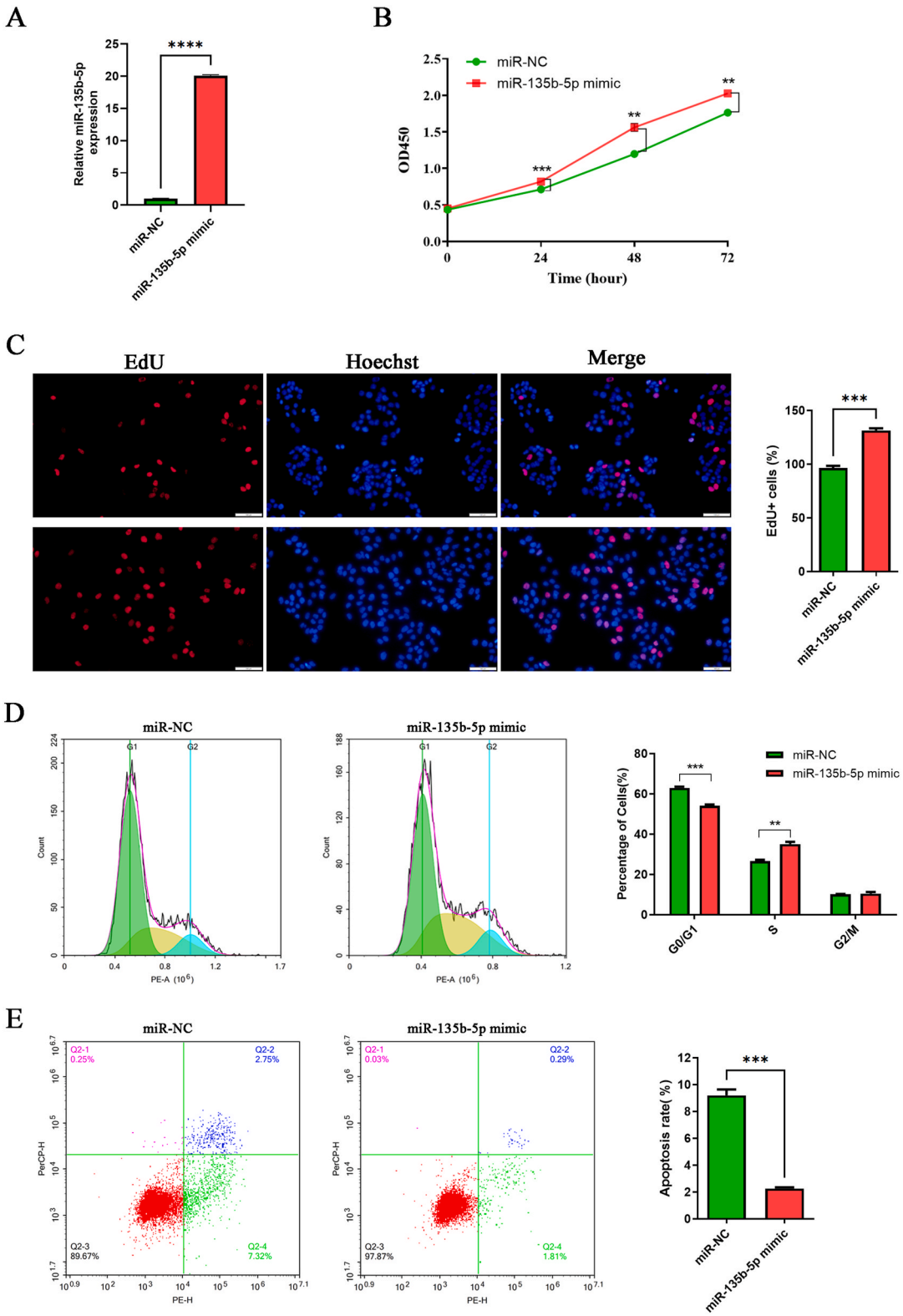

Fig. 7. miR-135b-5p promotes the growth of GCs. (A) Efficiency of miR-135b-5p expression in KGN cells transfected with miR-135b-5p mimic was verified by RT-qPCR. U6 was used for normalization. (B) The evaluation of cell viability by CCK-8 assays. (C) DNA synthesis capacity was determined by EdU assays. Scale bar = 100 μm. Cell cycle distribution (D) and the apoptotic rate (E) were analyzed by flow cytometry. $^{**}P < 0.01$, $^{***}P < 0.001$, $^{****}P < 0.0001$.

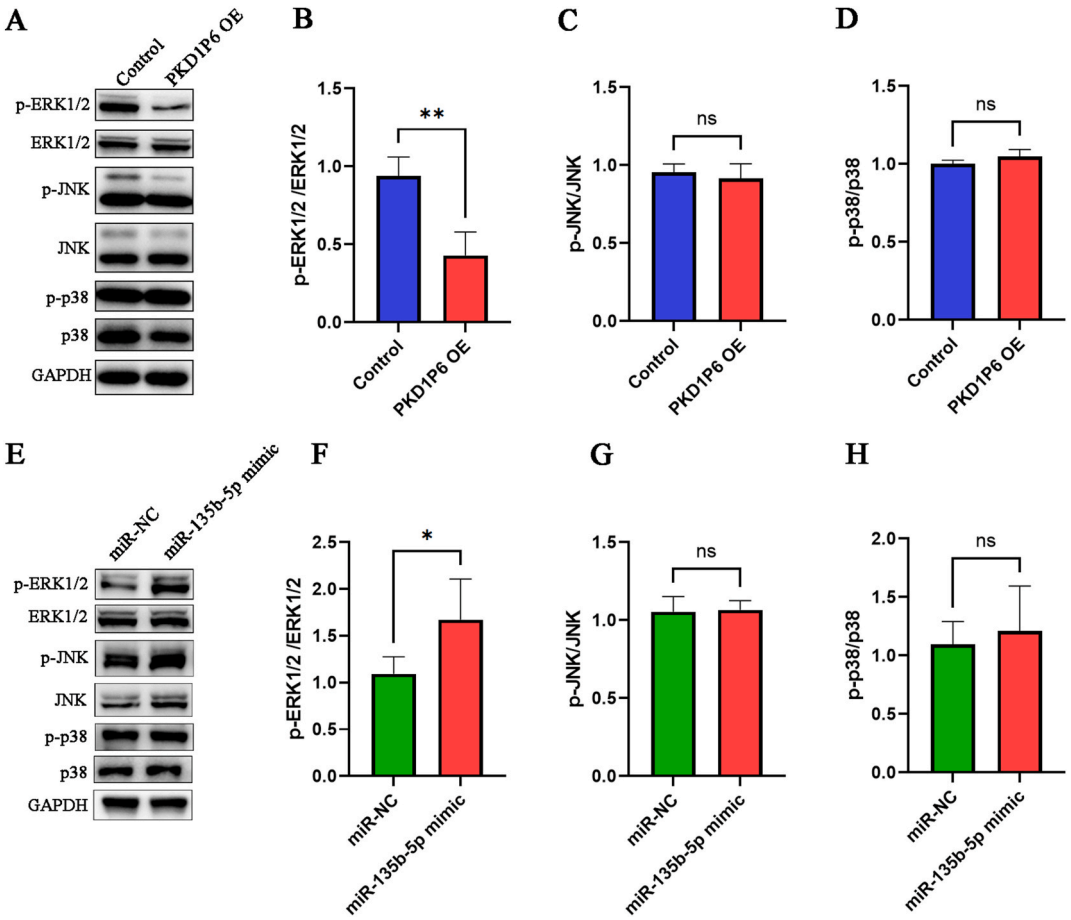

Fig. 8. PKD1P6/miR-135b-5p axis involves in regulating ERK1/2 signaling pathway. (A) Western blot analysis of protein expression levels of MAPK signaling molecules (p38, p-p38, JNK, p-JNK, ERK1/2, p-ERK1/2) in PKD1P6 overexpressed (OE) KGN cells. (B–D) Quantification of Western blot densitometry band via ImageJ software. (E) Western blot analysis of protein expression levels of MAPK signaling molecules in KGN cells transfected with miR-135b-5p mimic. (F–H) Quantification of Western blot densitometry band. $^{*}P < 0.05$, $^{**}P < 0.01$. ns: no significant difference.

therapies of HA-PCOS.

Funding

This study was supported by National Natural Science Foundation of China (No.81871161) and Fujian Provincial Health Technology Project (No.2023GGB01).

Ethics statement

The collection and use of all clinical samples in this study were approved by Ethics Committee of the First Affiliated Hospital of Xiamen University, and informed consent was obtained from all participants. The study was performed in accordance with the principles of the Declaration of Helsinki. Animal studies in this paper were approved by the Ethics Committee on Animal Experiments at Xiamen University.

Data availability statement

The data that support the findings of this study are available from the corresponding authors upon reasonable request.

CRediT authorship contribution statement

Weidong Zhou: Conceptualization, Data curation, Funding acquisition, Investigation, Methodology, Project administration, Supervision, Writing – original draft, Writing – review & editing. **Yikai Lian:** Investigation, Methodology, Validation. **Jiahao Chen:**

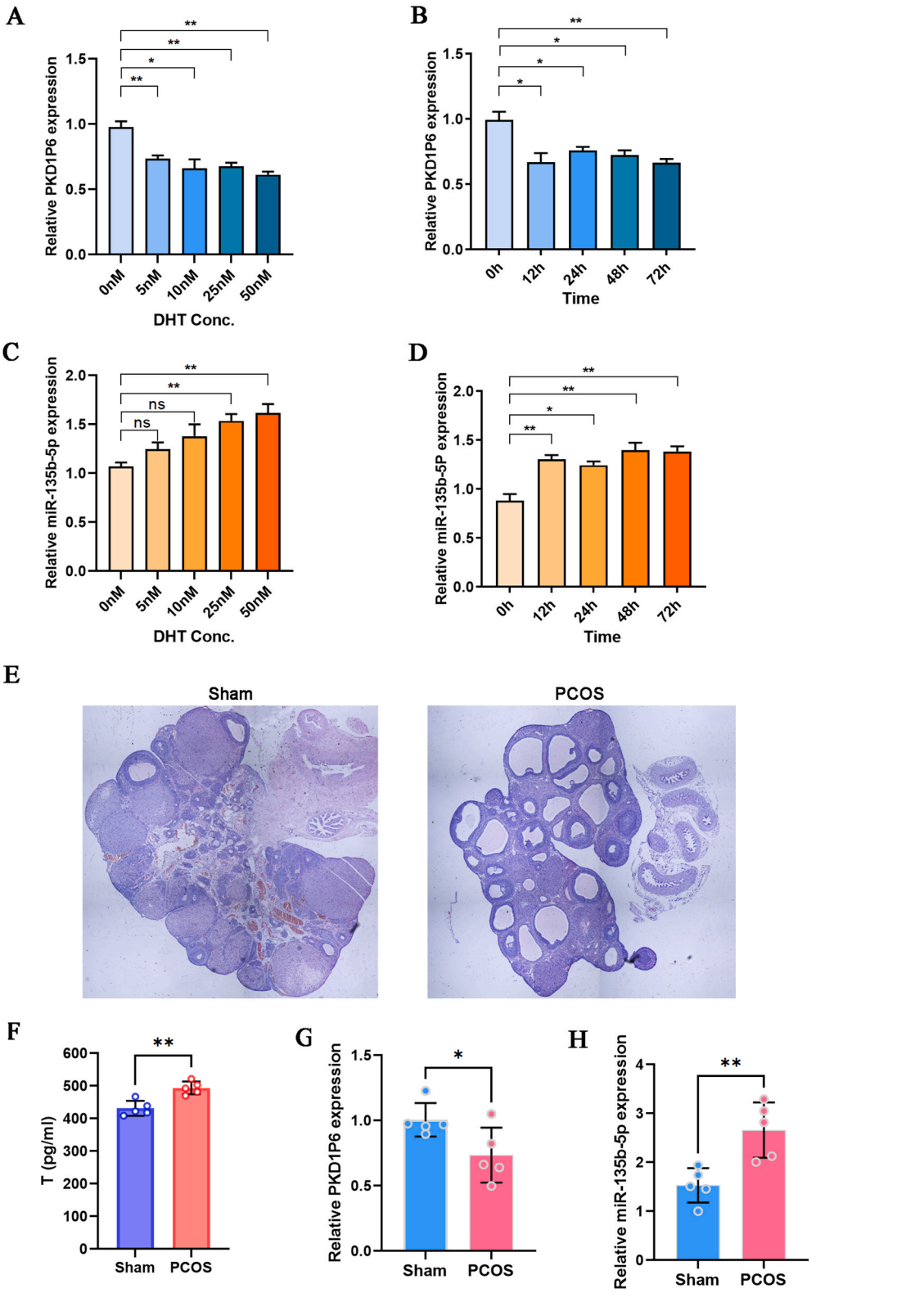

(caption on next page)

Fig. 9. Effects of excessive androgen on the expressions of PKD1P6 and miR-135b-5p in vitro and vivo. (A) Relative expression levels of PKD1P6 in KGN cells stimulated by DHT for 24 h were determined by RT-qPCR with dose-response experiments. (B) Relative expression levels of PKD1P6 in KGN cells stimulated by DHT (50 nM) were determined by RT-qPCR with time-response experiments. (C) Relative expression levels of miR-135b-5p in KGN cells stimulated by DHT for 24 h were determined by RT-qPCR with dose-response experiments. (D) Relative expression levels of miR-135b-5p in KGN cells stimulated by DHT (50 nM) were determined by RT-qPCR with time-response experiments. (E) Representative Hematoxylin and Eosin (H&E) staining images of ovaries in letrozole-induced PCOS rat models and the control group (Sham). (F) Serum testosterone (T) levels were detected by the enzyme linked immunosorbent assay (ELISA). (G–H) Expressions of PKD1P6 and miR-135b-5p in rat ovaries were detected by RT-qPCR. GAPDH or U6 was used for normalization. $*P < 0.05$, $**P < 0.01$. ns: no significant difference.

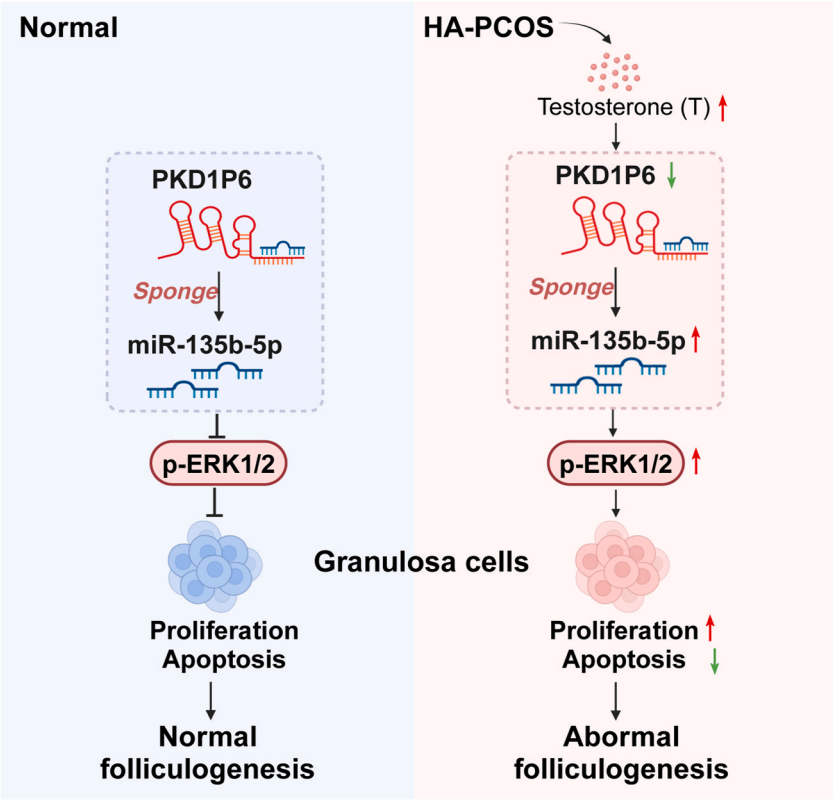

Fig. 10. Schematic diagram of PKD1P6 modulating ovarian granulosa cells (GCs) survival in abnormal folliculogenesis of HA-PCOS.

Investigation, Methodology, Validation. **Teng Zhang:** Investigation, Methodology, Validation. **Wenjing Zhang:** Methodology, Validation. **Ruofan Huang:** Methodology, Validation. **Mengjie Yang:** Methodology, Visualization. **Xiaohong Yan:** Methodology, Resources. **Qionghua Chen:** Data curation, Project administration, Resources, Supervision.

Declaration of competing interest

The authors declare that they have no known competing financial interests or personal relationships that could have appeared to influence the work reported in this paper.

Appendix A. Supplementary data

Supplementary data to this article can be found online at https://doi.org/10.1016/j.heliyon.2024.e36321.

References

[1] J.A. Visser, The importance of metabolic dysfunction in polycystic ovary syndrome, Nature reviews, Endocrinology 17 (2) (2021) 77–78.
[2] H.J. Teede, M.L. Misso, M.F. Costello, A. Dokras, J. Laven, L. Moran, T. Piltonen, R.J. Norman, P.N. International, Recommendations from the international evidence-based guideline for the assessment and management of polycystic ovary syndrome, Fertil. Steril. 110 (3) (2018) 364–379.

[3] R. Azziz, E. Carmina, Z. Chen, A. Dunaif, J.S. Laven, R.S. Legro, D. Lizneva, B. Natterson-Horowtiz, H.J. Teede, B.O. Yildiz, Polycystic ovary syndrome, Nat. Rev. Dis. Prim. 2 (2016) 16057.
[4] H.F. Escobar-Morreale, Polycystic ovary syndrome: definition, aetiology, diagnosis and treatment, Nat. Rev. Endocrinol. 14 (5) (2018) 270–284.
[5] C. He, K. Wang, Y. Gao, C. Wang, L. Li, Y. Liao, K. Hu, M. Liang, Roles of noncoding RNA in reproduction, Front. Genet. 12 (2021) 777510.
[6] L. Statello, C.J. Guo, L.L. Chen, M. Huarte, Author Correction: gene regulation by long non-coding RNAs and its biological functions, Nat. Rev. Mol. Cell Biol. 22 (2) (2021) 159.
[7] K.S. Liu, T.P. Li, H. Ton, X.D. Mao, Y.J. Chen, Advances of long noncoding RNAs-mediated regulation in reproduction, Chin Med J (Engl) 131 (2) (2018) 226–234.
[8] Y.D. Liu, Y. Li, S.X. Feng, D.S. Ye, X. Chen, X.Y. Zhou, S.L. Chen, Long noncoding RNAs: potential regulators involved in the pathogenesis of polycystic ovary syndrome, Endocrinology 158 (11) (2017) 3890–3899.
[9] J. Jiao, B. Shi, T. Wang, Y. Fang, T. Cao, Y. Zhou, X. Wang, D. Li, Characterization of long non-coding RNA and messenger RNA profiles in follicular fluid from mature and immature ovarian follicles of healthy women and women with polycystic ovary syndrome, Hum. Reprod. 33 (9) (2018) 1735–1748.
[10] W. Zhou, T. Zhang, Y. Lian, W. Zhang, M. Yang, Y. Li, L. Wang, X. Yan, Exosomal lncRNA and mRNA profiles in polycystic ovary syndrome: bioinformatic analysis reveals disease-related networks, Reprod. Biomed. Online 44 (5) (2022) 777–790.
[11] K. Hummitzsch, R.A. Anderson, D. Wilhelm, J. Wu, E.E. Telfer, D.L. Russell, S.A. Robertson, R.J. Rodgers, Stem cells, progenitor cells, and lineage decisions in the ovary, Endocr. Rev. 36 (1) (2015) 65–91.
[12] J. Tu, A.H. Cheung, C.L. Chan, W.Y. Chan, The role of microRNAs in ovarian granulosa cells in Health and disease, Front. Endocrinol. 10 (2019) 174.
[13] L.J. Webber, S.A. Stubbs, J. Stark, R.A. Margara, G.H. Trew, S.A. Lavery, K. Hardy, S. Franks, Prolonged survival in culture of preantral follicles from polycystic ovaries, J. Clin. Endocrinol. Metab. 92 (5) (2007) 1975–1978.
[14] J. Tu, Y. Chen, Z. Li, H. Yang, H. Chen, Z. Yu, Long non-coding RNAs in ovarian granulosa cells, J. Ovarian Res. 13 (1) (2020) 63.
[15] B. Xu, Y.W. Zhang, X.H. Tong, Y.S. Liu, Characterization of microRNA profile in human cumulus granulosa cells: identification of microRNAs that regulate Notch signaling and are associated with PCOS, Mol. Cell. Endocrinol. 404 (2015) 26–36.
[16] Y. Nishi, T. Yanase, Y. Mu, K. Oba, I. Ichino, M. Saito, M. Nomura, C. Mukasa, T. Okabe, K. Goto, R. Takayanagi, Y. Kashimura, M. Haji, H. Nawata, Establishment and characterization of a steroidogenic human granulosa-like tumor cell line, KGN, that expresses functional follicle-stimulating hormone receptor, Endocrinology 142 (1) (2001) 437–445.
[17] C. Thery, S. Amigorena, G. Raposo, A. Clayton, Isolation and characterization of exosomes from cell culture supernatants and biological fluids, Curr Protoc Cell Biol Chapter 3 (2006). Unit 3 22.
[18] J.S. Nasser, N. Altahoo, S. Almosawi, A. Alhermi, A.E. Butler, The role of MicroRNA, long non-coding RNA and circular RNA in the pathogenesis of polycystic ovary syndrome: a literature review, Int. J. Mol. Sci. 25 (2) (2024).
[19] S.A. Stubbs, J. Stark, S.M. Dilworth, S. Franks, K. Hardy, Abnormal preantral folliculogenesis in polycystic ovaries is associated with increased granulosa cell division, J. Clin. Endocrinol. Metab. 92 (11) (2007) 4418–4426.
[20] M. Das, O. Djahanbakhch, B. Hacihanefioglu, E. Saridogan, M. Ikram, L. Ghali, M. Raveendran, A. Storey, Granulosa cell survival and proliferation are altered in polycystic ovary syndrome, J. Clin. Endocrinol. Metab. 93 (3) (2008) 881–887.
[21] W. Strzalka, A. Ziemienowicz, Proliferating cell nuclear antigen (PCNA): a key factor in DNA replication and cell cycle regulation, Ann. Bot. 107 (7) (2011) 1127–1140.
[22] Q. Wang, G. He, M. Hou, L. Chen, S. Chen, A. Xu, Y. Fu, Cell cycle regulation by alternative polyadenylation of CCND1, Sci. Rep. 8 (1) (2018) 6824.
[23] A. Karimian, Y. Ahmadi, B. Yousefi, Multiple functions of p21 in cell cycle, apoptosis and transcriptional regulation after DNA damage, DNA Repair 42 (2016) 63–71.
[24] M. Abbastabar, M. Kheyrollah, K. Azizian, N. Bagherlou, S.S. Tehrani, M. Maniati, A. Karimian, Multiple functions of p27 in cell cycle, apoptosis, epigenetic modification and transcriptional regulation for the control of cell growth: a double-edged sword protein, DNA Repair 69 (2018) 63–72.
[25] B. Alipoor, S. Nikouei, F. Rezaeinejad, S.N. Malakooti-Dehkordi, Z. Sabati, H. Ghasemi, Long non-coding RNAs in metabolic disorders: pathogenetic relevance and potential biomarkers and therapeutic targets, J. Endocrinol. Invest. 44 (10) (2021) 2015–2041.
[26] L. Salmena, L. Poliseno, Y. Tay, L. Kats, P.P. Pandolfi, A ceRNA hypothesis: the Rosetta Stone of a hidden RNA language? Cell 146 (3) (2011) 353–358.
[27] D. Yuan, J. Luo, Y. Sun, L. Hao, J. Zheng, Z. Yang, PCOS follicular fluid derived exosomal miR-424-5p induces granulosa cells senescence by targeting CDCA4 expression, Cell. Signal. 85 (2021) 110030.
[28] Z. Zhou, Z. Tu, J. Zhang, C. Tan, X. Shen, B. Wan, Y. Li, A. Wang, L. Zhao, J. Hu, N. Ma, J. Zhou, L. Chen, Y. Song, W. Lu, Follicular fluid-derived exosomal MicroRNA-18b-5p regulates PTEN-mediated PI3K/Akt/mTOR signaling pathway to inhibit polycystic ovary syndrome development, Mol. Neurobiol. 59 (4) (2022) 2520–2531.
[29] R. Roskoski Jr., ERK1/2 MAP kinases: structure, function, and regulation, Pharmacol. Res. 66 (2) (2012) 105–143.
[30] S. Huang, Y. Pang, J. Yan, S. Lin, Y. Zhao, L. Lei, L. Yan, R. Li, C. Ma, J. Qiao, Fractalkine restores the decreased expression of StAR and progesterone in granulosa cells from patients with polycystic ovary syndrome, Sci. Rep. 6 (2016) 26205.
[31] N. Zhang, X. Liu, L. Zhuang, X. Liu, H. Zhao, Y. Shan, Z. Liu, F. Li, Y. Wang, J. Fang, Berberine decreases insulin resistance in a PCOS rats by improving GLUT4: dual regulation of the PI3K/AKT and MAPK pathways, Regul. Toxicol. Pharmacol. 110 (2020) 104544.